Single-shot phase retrieval with complex diversity

AKIRA EGUCHI*, TOM D. MILSTER

College of Optical Sciences, The University of Arizona, 1630 E. University Blvd. Tucson, AZ 85721, USA
**Corresponding author: akiraeguchi@optics.arizona.edu*

Received XX Month XXXX; revised XX Month, XXXX; accepted XX Month XXXX; posted XX Month XXXX (Doc. ID XXXXX); published XX Month XXXX

The concept of complex diversity is introduced that adequately accounts for special considerations in the design of the system and the reconstruction algorithm for single-shot phase retrieval techniques. Complex-number pupil filters containing both amplitude and phase values are extracted by numerical propagation from a computer-generated hologram design, which generates multiple images in a single acquisition. The reconstruction is performed by a Fourier iterative algorithm modified with an area restriction to avoid noise amplification. Numerical simulations show that the complex diversity technique estimates extrinsic Kolmogorov aberration better than conventional single-shot techniques for a distant point object. Experiments show that sensor-less adaptive optics correction is achieved using the complex diversity technique.

http://dx.doi.org/10.1364/OL.xx.xxxxxx

1. Introduction

Phase retrieval is a technique to measure unknown extrinsic phase disturbances, which is attractive because of its simplicity compared to more complicated systems that involve interferometers or Shack-Hartmann sensors [1,2]. Phase retrieval drawbacks include the requirement of multiple image acquisitions ("shots"), low accuracy, and stagnation issues. Some of these issues have been overcome by single-shot phase retrieval associated with various diversities [3–5]. These single-shot techniques effectively achieve multiple image acquisitions with different phase diversity values through the use of special gratings designed to generate multiple diffraction orders that are detected simultaneously in a single image acquisition. In either multiple-shot or single-shot techniques, each measurement is characterized by the filter applied to the pupil of the optical system that modifies the image distribution. For example, focus diversity applies quadratic phase filters with different peak phase values to each measurement. This filter must be known precisely for accurate extrinsic phase reconstruction. However, for single-shot techniques, the effective filter applied to the diffracted orders and an accurate reconstruction algorithm that utilizes the effective filters have not been adequately discussed. In this paper, accurate effective filters are determined in a new diversity concept called complex diversity for single-shot phase retrieval, and an associated reconstruction algorithm is proposed.

The original phase retrieval algorithm is credited to Gerchberg and Saxton in 1972 [1], and Fienup generalized this algorithm by using finite support and non-negativity constrains [2]. In subsequent years, accuracy and convergence were improved by implementing several different diversities, such as defocus diversity [6,7], translation diversity [8], shifting illumination [9], and random diversity [10,11]. However, these diversity techniques generally require multiple shots.

Recently, single-shot phase retrieval techniques with special gratings have overcome this multiple-shot issue. Blanchard et al. pioneered the single-shot technique with a distorted grating that introduces defocus into +/-1 diffraction orders [3]. Then, straightforward implementation without energy loss was proposed with a spatial light modulator (SLM) [12]. Other diversity techniques, like translation diversity [4], multiple illumination [5], and weakly scattering phase [13], were also realized with single-shot techniques by implementing Dammann gratings. Yao et al. also proposed a new phase grating designed to introduce different transmittance filters into the diffracted orders [14].

Phase gratings and computer-generated holograms (CGHs) are attractive for distribution of multiple images on a camera plane in a single shot because they create multiple orders without power loss and are easily implemented with a SLM. However, the true effective filters applied to individual diffraction orders are not obvious. Even though the CGHs are designed from seed filter patterns, the true effective filters are not the same as the seed filters, because the complex field modulation is not constrained in the design process, as explained below. The reconstruction process requires accurate knowledge of the effective filters for each diffraction order for high quality reconstruction of the extrinsic phase.

In this study, a new diversity concept is proposed to achieve accurate phase retrieval with a single-shot acquisition. Multiple irradiance data are obtained by a CGH designed to generate multiple diffraction orders with different diversity values. The effective filters associated with the individual diffraction orders from the CGH are calculated. It is demonstrated that the effective filters are extracted by numerical propagation, and they must include both real and imaginary values, which signify both absorption and phase shift versus position in the filter plane, rather than the common practice of specifying only the phase portion of the filter. We categorize this new concept of phase retrieval with complex effective filters as complex diversity. A modified classical Fourier iterative algorithm is used for reconstruction of the extrinsic aberration in order to avoid noise amplification due to small amplitudes of the effective filters. The new diversity technique is evaluated by numerical simulations, and preliminary adaptive optics (AO) experiments with a synthetic extrinsic aberration and a liquid crystal on silicon (LCoS) SLM.

This paper consists of the following sections. Section 2 describes the concept and the principle of complex diversity. Section 3 describes simulation results, which indicate that the complex diversity technique estimates extrinsic aberration better than the conventional phase-only single-shot technique. Section 4 shows experimental results. Section 5 lists primary conclusions from this work.

2. Principle

A. Concept of complex diversity

Conventional phase diversity techniques measure multiple irradiance images with different filters in the pupil plane, as shown in Fig. 1(a). Following Gerchberg's notation, the series of different irradiance images generated from different phase filters are called phasorgrams [15,16]. In this study, the CGH generates multiple diffraction orders with different effective filters that create multiple images at different positions on an image sensor, as shown in Fig. 1(b). By dividing the image, multiple phasorgrams are obtained from a single image acquisition. In conventional phase diversity reconstruction algorithms, phase filters corresponding to the phasorgrams are the same as the ones used to generate the phasorgrams. On the other hand, optimum effective filters for reconstruction are not obvious in single-shot techniques, since they require both amplitude and phase information. The following sub-sections describe design of the CGH, extraction of the effective filters, and the modified reconstruction algorithm.

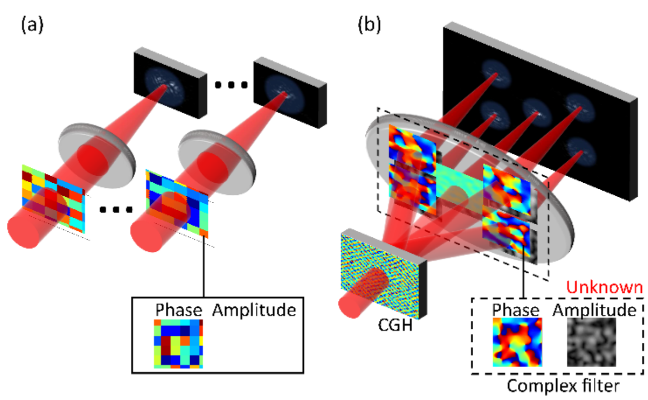

Fig. 1. A concept of the complex diversity. (a) Conventional diversity, (b) Complex diversity.

B. CGH Design

Our phase retrieval technique consists of three steps, as illustrated in Fig. 2. The first step is design of the CGH, which starts with setting up N seed filters that are proper for determining an extrinsic aberration. In principle, arbitrary modulations can be used as the seed filters. In this study, random phase seed filters are selected, because they show better performance for estimating Kolmogorov extrinsic disturbances than other forms of diversity [16]. Especially for single-shot techniques, it is important to keep the dynamic range of signal values for all phasorgrams at nearly the same levels, because exposure time and incident light power cannot be adjusted for the individual phasorgrams. With random phase diversity, generated phasorgrams exhibit similar peak values, unlike defocus diversity. The seed filters are converted to complex field phasorgrams by inverse fast Fourier transforms $\boldsymbol{F}_\xi^{-1}[\ ]$. Amplitudes of the complex fields of the N individual phasorgrams are mapped onto different positions in the image plane. This multiple-phasorgram amplitude distribution is the target amplitude for the CGH design. Conventional CGH design techniques, such as the Gerchberg-Saxton (GS) algorithm [1] and modified GS technique [17], can be used for this design. Constraints in the CGH design include a pure phase constraint in the pupil plane and the amplitude target distribution in the image plane. The designed CGH is displayed on the LCoS during the measurement.

C. Extraction of effective filters

The second step is extraction of the N complex effective filters. Although the CGH generates the same amplitude patterns as generated from individual seed filters, the field modulations introduced into the diffraction orders are not the same as the seed filters of the CGH, because the CGH design process does not constrain these field modulations. Thus, the actual effective filters must be extracted from the designed CGH.

The complex field reflected from the CGH pattern is calculated in a computer by assuming illumination with a uniform plane-wave amplitude. Then, the field is numerically propagated to the image plane by $\boldsymbol{F}_\xi^{-1}[\ ]$. The complex field at the image plane is divided into N individual subareas corresponding to the phasorgrams by cropping data in the image plane, which results in a collection of phasorgrams. The phasorgram fields from the cropped subareas are individually propagated back to the pupil plane with fast Fourier transforms $\boldsymbol{F}_x[\ ]$. The resulting collection of N complex field patterns in the pupil plane are the effective filters; A_i, and ϕ_i (i=1:N), introduced to the individual diffraction orders. The design process and the extraction process are performed only one time when a new CGH is generated. Thus, these additional process steps do not increase computational time for the reconstruction.

D. Reconstruction algorithm

The third step is reconstruction. The experimentally measured single-shot irradiance pattern using the CGH and the extrinsic aberration ϕ_{ex} is divided into N individual phasorgrams I_i, which are used in the reconstruction. The reconstruction algorithm in this study is an iterative Fourier method with field averaging proposed by Gerchberg [15,16], which is modified for complex diversity. It starts with setting an initial guess in the pupil plane as a flat phase, i.e. no aberration $\phi_{ex}(1) = 0$, for the extrinsic phase and with unit amplitude $A_s(1)$=1. Then, the following steps proceed in an iterative manner. (i) The effective filters are applied to yield N individual pupil fields by multiplying the complex transmission of the effective filter $A_i\exp(j\phi_i)$ by the estimate of the extrinsic phase distribution $\overline{U_s}(k) = A_s(k)\exp[j\phi_{ex}(k)]$, where k is the number of iterations, and pupil-plane values are indicated with a subscript s. (ii) $\boldsymbol{F}_x[\ ]$ generate N individual complex fields on the image plane. (iii) An amplitude constraint is applied by replacing the calculated amplitudes with the square root of the measured phasorgram set $\sqrt{I_i}$, while maintaining the calculated phase. (iv) $\boldsymbol{F}_\xi^{-1}[\ ]$ are applied to the N fields to propagate them back to the pupil plane. (v) The resulting complex pupil fields are divided by the complex transmission of the effective filters, in order to form N individual estimates of the extrinsic phase. (vi) These N estimates are averaged to obtain the iteration's final estimate of the extrinsic field, except in areas where amplitudes of the effective filters are smaller than a threshold value to avoid noise amplification ($\sum'/N'$). In this study, the threshold value is set to 10% of the maximum amplitude. The process from (i) to (vi) is defined as one iteration, and iterations are repeated until the mean error $\bar{\varepsilon}$ between the measured irradiance pattern and the synthetically generated irradiance pattern falls below a target threshold value, or the iteration number reaches a pre-determined maximum. After the final estimate for ϕ_{ex} is retrieved, the complex conjugate of the retrieved phase ($-\phi_{ex}$) is displayed on the LCoS to achieve AO correction for compensation of the extrinsic aberration.

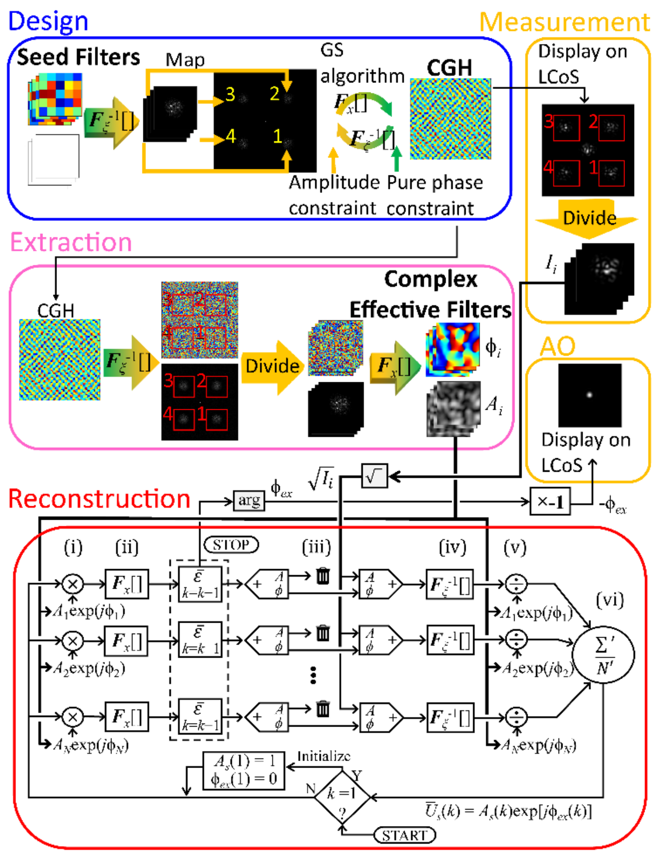

Fig. 2. Algorithm of single-shot phase retrieval with the complex diversity, and AO correction.

3. Simulation

To match the experimental conditions, simulations are run in which the wavelength λ is 632.8 nm and the image side NA is 0.01. The pixel size of the 1280 x 1024 image sensor is 5.2 µm. A synthetic Kolmogorov phase disturbance, which is applicable in astronomy [18] and biological imaging [19], is the extrinsic aberration, as shown in Fig. 3(a). It is generated from approximated Kolmogorov's power spectrum that follows a -11/3 power law [20]. The seed filters for the CGH design are random phase patterns with super-pixel segments, and $N = 4$ [16]. The CGH is designed by the modified GS algorithm [17] with the amplitude constraint at the image plane generated from the seed filters, and a pure phase constraint is implemented at the pupil plane. The effective filters are extracted from the designed CGH as described in Section 2.

Fig. 3(b) shows a simulated irradiance pattern in the image plane. The reconstruction is performed with both the effective filters and the seed filters to show the improvement using complex diversity. Comparisons are made with different separations between 0th and 1st order diffraction orders, as indicated by L in Fig. 3(b), different sizes of the super-pixels $L_s = D/5$, $D/16$, and $D/32$ on a side, and where D is the diameter of the incident beam at the pupil plane. Fig. 3(c) shows retrieved phases with $L_s = D/16$. The top row contains retrieved phases by the complex diversity technique with different L values, and the bottom row shows retrieved phases with the conventional diversity technique. As compared with the reference extrinsic aberration shown in Fig. 3(a), complex diversity subjectively performs better than conventional diversity.

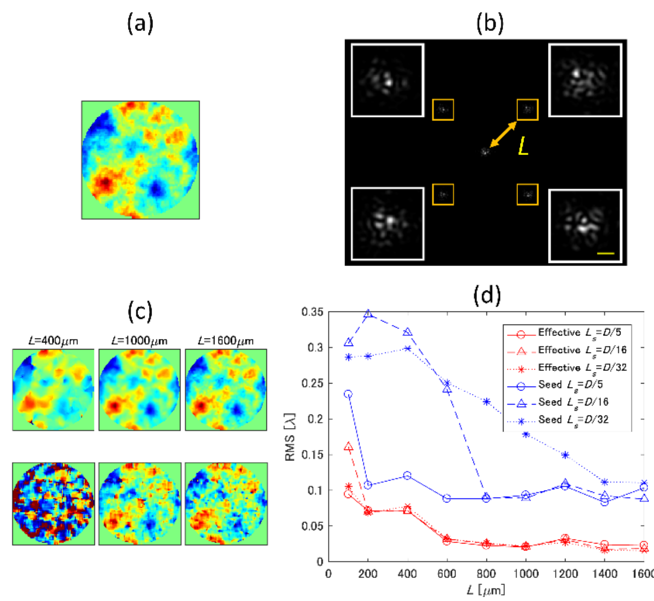

Fig. 3. Simulation results. (a) An extrinsic Kolmogorov aberration. (b) A simulated irradiance pattern at the image plane. The scalebar shows 100 µm. (c) Retrieved aberrations with $L_s = D/16$. The effective filters (top) and the seed filters (bottom). (d) Residual RMS.

Fig. 3(d) shows residual errors of the estimated aberrations. The residuals are evaluated by the root mean square (RMS) of the residual phase between the reference phase and the estimated phase. Complex diversity exhibits from 1.5 to 8.6 times lower RMS values than conventional diversity, and the improvements are relatively greater with shorter L. As shown in reference [16], the array of super-pixels with period L_s of the seed random phase patterns results in a maximum range of light scattering at the image plane of

$$D_{samp} = \frac{1}{2}\frac{\lambda}{NA}\frac{D}{L_s}, \quad (1)$$

where λ is wavelength, and NA is numerical aperture on the image side. D_{samp} are calculated as 158 µm, 506 µm, and 1013 µm for $L_s = D/5$, $D/16$, and $D/32$, respectively. As overlaps between phasorgrams increase for L shorter than D_{samp}, the RMS error increases and effective filter results differ more from reconstruction with the seed filters. When the light distributions overlap from different seed filters as L decreases, it becomes more difficult for the standard phase diversity technique to separate information about the extrinsic phase. Therefore, the complex diversity technique works better than the conventional diversity technique in the range of shorter L. In some applications, like imaging a star field with separated incoherent point sources, the separation L should be small to avoid overlaps between the phasorgram regions. In that case, the complex diversity technique has a significant advantage over using the seed filters in the reconstruction algorithm.

4. Experiment

The experimental setup is the same as the author's previously published research [16], which is a sensor-less geometry that does not require modification to use complex diversity. The extrinsic aberration is an artificial Kolmogorov phase plate generated by gray-scale lithography [21] placed in a plane conjugate to the LCoS. Incident light from HeNe laser illuminates the Kolmogorov phase plate, and the disturbed light is relayed to the LCoS. The CGH is displayed on the LCoS, and generated diffraction orders create multiple spots on the CMOS camera by an imaging lens. The CGH design process and the effective filter extraction process are the same as the simulation. The CGH is designed for spot separation L = 1600 μm on the image plane, and $L_s = D/5$. The reconstruction process estimates the extrinsic aberration from the measured single irradiance pattern, as described in Section 2. AO correction is achieved by displaying the complex conjugate of the retrieved aberration on the LCoS.

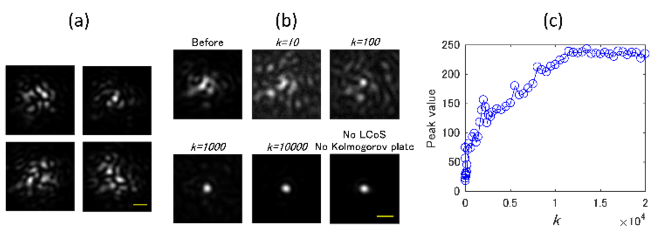

Fig. 4. Experimental results. (a) Four phasorgrams divided from a measured irradiance image. The scalebar shows 100 μm. (b) AO correction results. The top left is the image before correction, and the bottom right is the image without the LCoS and the artificial Kolmogorov phase plate. The others show the images corrected with the estimated phases at the iteration k. The scalebar shows 100 μm. (c) Peak values of the corrected spots.

Four diffracted orders are observed at the corners of a measured irradiance image. They are divided into four phasorgram subareas as shown in Fig. 4(a). Exposure time is adjusted to make the distributed phasorgrams within the dynamic range of the CMOS, even though the 0th order diffraction light is saturated. The extrinsic aberration is reconstructed from the four phasorgrams and the four effective filters. Fig. 4(b) shows corrected images with the estimated phases at iteration k. Before AO correction, a point image is totally disturbed due to the artificial Kolmogorov phase plate. As iterations increase, image quality is improved. After 10000 iterations, the corrected point images are almost identical to the image measured without the artificial Kolomogorov phase plate and the LCoS, which shows that the complex diversity technique works for sensor-less AO correction. As shown in Fig. 4(c), peak values of the corrected spots rise with more iterations, and they saturate after 10000 iterations. Retrieved phases are compared between the complex diversity technique and the conventional interferometric measurement, and reasonable matching is obtained.

5. Conclusion

In this study, a new phase retrieval technique called complex diversity is demonstrated, which produces multiple phasorgrams in a single-shot measurement using a CGH designed to generate multiple diffraction orders. Complex effective filters are extracted by numerical propagation from the CGH design. The reconstruction is performed with a Fourier iterative algorithm modified with an area restriction to avoid noise amplification. Improvement by the complex diversity technique is verified by numerical simulations and AO experiments. Numerical simulations show that the complex diversity technique estimates the extrinsic aberration better than conventional phase-only single-shot techniques, and the improvement is significant in the range of the small separation between 1st and 0th order diffraction spots. Experiments show that the complex diversity technique works for sensor-less single-shot AO correction.

Acknowledgments

We thank Canon Inc. for financial support. We are grateful to Professor Michael Hart, Lee Johnson and John Brewer for their technical support. We also thank for an equipment donation from the Arizona Technology and Research Initiative Fund (TRIF).

References

1. R. W. Gerchberg and W. O. Saxton, Optik (Stuttg). **35**, 237 (1972).
2. J. R. Fienup, Appl. Opt. **21**, 2758 (1982).
3. P. M. Blanchard, D. J. Fisher, S. C. Woods, and A. H. Greenaway, Appl. Opt. **39**, 6649 (2000).
4. X. Pan, C. Liu, and J. Zhu, Appl. Phys. Lett. **103**, 171105 (2013).
5. X. He, C. Liu, and J. Zhu, Opt. Lett. **43**, 214 (2018).
6. R. A. Gonsalves, Opt. Eng. **21**, 829 (1982).
7. B. H. Dean and C. W. Bowers, J. Opt. Soc. Am. A **20**, 1490 (2003).
8. G. R. Brady, M. Guizar-Sicairos, and J. R. Fienup, Opt. Express **17**, 624 (2009).
9. J. M. Rodenburg and H. M. L. Faulkner, Appl. Phys. Lett. **85**, 4795 (2004).
10. F. Zhang, G. Pedrini, and W. Osten, Phys. Rev. A **75**, 043805 (2007).
11. P. F. Almoro and S. G. Hanson, Appl. Opt. **47**, 2979 (2008).
12. B. Chen, X. Li, and X. Yang, Proc. SPIE 962015 (2015).
13. X. He, X. Pan, C. Liu, and J. Zhu, Appl. Opt. **57**, 4832 (2018).
14. Y. Yao, X. He, C. Liu, and J. Zhu, J. Microsc. **270**, 129 (2018).
15. R. W. Gerchberg, U.S. patent 6,906,839, (2005).
16. A. Eguchi, J. Brewer, and T. D. Milster, Appl. Opt. **58**, 6834 (2019).
17. J. Christmas and M. Keynes, U.S. patent application 2015/0022526, (2015).
18. R. K. Tyson and B. W. Frazier, *Field Guide to Adaptive Optics, 2nd ed.* (SPIE Press, 2012).
19. J. M. Schmitt and G. Kumar, Opt. Lett. **21**, 1310 (1996).
20. R. G. Lane, A. Glindemann, and J. C. Dainty, Waves in Random Media **2**, 209 (1992).
21. M. Zaverton, J. Sierchio, Y. S. Kim, D. Hansen, W. Bletcher, J. Tamkin, and T. D. Milster, in International Optical Design Conference and Optical Fabrication and Testing, (Optical Society of America, 2010), paper OTuC5.